An OGCM investigation of the Red Sea circulation. Part I.: The exchange between the Red Sea and the Indian Ocean

Sarantis S. Sofianos,[1]

RSMAS, University of Miami, Miami, Florida

William E. Johns

RSMAS, University of Miami, Miami, Florida

Short title: AN OGCM INVESTIGATION OF THE RED SEA CIRCULATION. PART I

Abstract.

The mechanisms involved in the seasonal exchange between the Red Sea and the Indian Ocean are studied using an Oceanic General Circulation Ocean Model, namely the Miami Isopycnic Coordinate Ocean Model (MICOM). The model reproduces the basic characteristics of the of the seasonal circulation observed in the area of the strait of Bab el Mandeb. There is good agreement between model results and available observations on the strength of the exchange and the characteristics of the water masses involved, as well as the seasonal flow pattern. During winter this flow consists of a typical inverse estuarine circulation while during summer the surface flow reverses, there is an intermediate inflow of relatively cold and fresh water, and the hypersaline outflow at the bottom of the strait is significantly reduced. Additional experiments with different atmospheric forcing (seasonal winds, seasonal thermohaline air-sea fluxes, or combinations) were performed in order to assess the role of the atmospheric forcing fields in the exchange flow at Bab el Mandeb. The results of both the wind- and thermohaline-driven experiments exhibit a strong seasonality at the area of the strait which is in phase with the observations. But it is the combination of both the seasonal pattern of the wind-stress and the seasonal thermohaline forcing that can reproduce the observed seasonal variability at the strait. The importance of the seasonal cycle of the thermohaline forcing on the exchange flow pattern is also emphasized by these results. In the experiment where the thermohaline forcing is represented by its annual mean, the strength of the exchange is reduced almost by half.

Introduction

The Red Sea is an elongated basin separating the African and Asian continents, extending from $12.5^o N$ to $30^o N$ (a distance of about 2000 km) with an average width of 220 km (Patzert,1974a). The surface area of the Red Sea is $4.5 \times 10^{11} m^2$ and the mean depth 524 m (Patzert, 1974a), but with maximum recorded depths of almost 3000 m. At the northern end it bifurcates into two gulfs, the Gulf of Suez with average depth of 40 m and the Gulf of Aqaba with depths exceeding 1800 m and a sill at the entrance of approximately 175 m (Neumann and Gill, 1962). The transport through the Suez Cannal, which connects the Mediterranean Sea with the Gulf of Suez and the Red Sea, is extremely small. Therefore, the only significant connection between the Red Sea and the open ocean is the strait of Bab el Mandeb located at the southern end of the basin, which connects to the Gulf of Aden and Indian Ocean. It is a shallow and narrow channel with a sill depth of 160 m and a minimum width of about 25 km.

Due to the excess evaporation, the Red Sea is a typical concentration basin and an inverse estuarine circulation is expected at the strait of Bab el Mandeb, with a relatively fresh surface inflow on the top of a deep outflow of higher salinity water. For more than a century the general idea among the scientists investigating the region was that a two layer exchange must persist throughout the year, like in the case of the Mediterranean Sea and the Gibraltar strait (Maury, 1855; Schott, 1929). This idea was supported by several observational attempts, all of them taking place during the winter months (October to May) (Luksch, 1901; Krümmel, 1911; Vercelli, 1927). It was in July 1929, when an Italian expedition on board the AMIRAGLIO MAGNAGHI carried out current measurements along the strait, that Vercelli (1931) for the first time demonstrated the presence of a three-layer exchange during the summer, with surface and deep outflows and an intermediate inflowing layer. Later observations (Sewell, 1934; Thompson, 1939b; Maillard and Soliman, 1986) supported the existence of this kind of seasonal variability as a permanent feature of the exchange between the Red Sea and the Indian Ocean. The overall picture emerging from all available investigations in the area is a two-layer winter inverse estuarine (fresh inflow on top of a hypersaline outflow) exchange during October to May, replaced between June and September by a three-layer exchange comprised of a shallow surface outflow, an intermediate intrusion of the relatively fresh and cold Gulf of Aden Intrusion Water mass (GAIW), and a deep hypersaline outflow which is a small fraction of the winter value.

The explanation of the exchange flow and its variability must include consideration of the forcing and dynamics governing the whole region (the system Red Sea - Strait - Gulf of Aden). Although all previous studies agree that the evaporation over the Red Sea far exceeds the precipitation, the actual $E - P$ rate is highly debated, ranging in the available literature from 1.5 to 2.3 $m/year$ (Yegorov, 1950; Neumann, 1952; Privett, 1959; da Silva, 1994; Tragou et al., 1999). The annual mean heat flux from the surface of the Red Sea is very small (Patzert, 1974b) but the seasonal variability is important with an annual cycle of more than $200\,Wm^{-2}$ range (Tragou et al., 1999). Recent observations (Murray and Johns, 1997) have made possible an accurate estimation of the annual mean fresh water and heat budgets of the Red Sea (Sofianos et al., 2001) producing an $E - P$ rate of $2.06 \pm 0.22\, m/year$ and a heat loss of approximately $11 \pm 5\, Wm^{-2}$ from the surface of the sea. The wind field is also strong and exhibits considerable seasonality (Patzert, 1974a). In the northern part of the Red Sea the climatological winds are from the northwest throughout the year but in the southern part of the basin, influenced by the Indian Monsoon, they reverse annually from southeast during winter to northwest during summer (June to September).

Although there is a general agreement that both thermohaline and wind forcing play a role in generating the horizontal and vertical circulation, the stratification of the area, and the exchange at Bab el Mandeb, the relative importance of each one and the role they play are highly disputed. The different theories that evolved during the last century ignore in general one or the other forcing mechanism and emphasize either the mean exchange or its seasonal variability. The buoyancy loss has been thought by several investigators to be the basic controlling mechanism of the flow (Maury, 1855; Luksch, 1901; Neumann and McGill, 1962; Phillips, 1966). Others believe that the wind-stress field is more important in determining the circulation pattern (Thompson, 1939a; Siedler, 1969; Patzert, 1974a).

The most representative theory of the thermohaline-driven circulation of the Red Sea is by Phillips (1966), involving similarity solutions of a convectively driven model. He assumed a semi-enclosed basin, with a sill and constant width, so that the circulation is in the vertical plane and no rotational effect is present. The model is driven by a uniform buoyancy loss over the surface of the basin and the circulation is in steady state. The circulation produced by the model is a two-layer flow and the exchange at the sill is in qualitative agreement with the observed winter pattern.

A very different approach was pursued by Patzert (1974a) for explaining the mechanisms behind the basic circulation features observed in the Red Sea and the exchange with the Indian Ocean. Based on the obvious coincidence of the reversal of the the wind field in the southern Red Sea with the reversal of the surface flow in the strait, he hypothesized that the variable wind-stress and the associated changes of the sea level in the southern Red Sea and the Gulf of Aden control the circulation in the region throughout the year and the exchange flow at the strait of Bab el Mandeb. To explain the three-layer system present during summer, Patzert proposed that the northwest winds and a drop in the sea level at the northwestern Gulf of Aden due to wind-induced upwelling force a shallow surface layer outflow from the basin. The same mechanism displaces the subsurface isopycnals upward, producing an opposite pressure gradient at intermediate depths that induces the intermediate intrusion of GAIW. The relative importance of the direct wind-stress effect and the indirect effect through sea level setup across the strait were not determined, however.

During the past century very few studies were carried out to measure directly the exchange flow at Bab el Mandeb and most of them were very short term lasting for only a few days to a few months (Vercelli, 1927; Siedler, 1968; Maillard and Soliman, 1986). In order to assess the annual mean strength of the exchange and the seasonal variability most investigators have used indirect methods. Patzert (1974b) put together ship's drift observations from the Koniklijk Nederlands Meteorologisch Instituut (KNMI,1949)

Atlas and hydrographic data at the strait to estimate the seasonal cycle of the exchange flow. He calculated the monthly mean transports for a two-layer exchange (Table 1), using a 0.03 Sv adjustment for the lower layer to account for the freshwater loss inside the basin due to $E - P$, and assuming that the summer deep outflow was negligible. Using an evaporation rate of about 2.1 $m/year$ he estimated the annual mean surface transport to be 0.33 Sv and the outflow of the saline Red Sea Outflow Water (RSOW) to be 0.30 Sv. Siedler (1969) used an $E - P$ value of 2 $m/year$ and average salinities for a two-layer exchange in Knudsen's formula (Knudsen, 1900) to estimate an annual mean RSOW outflow of 0.33 Sv. Finally, Bethoux (1987) used the same method and salinity values but with 2.4 $m/year$ of $E - P$ and an annual cycle around this annual mean value, estimated by Hasternath and Lamb (1979), to get a mean RSOW outflow of 0.38 Sv. The annual cycle of the exchange flow from Bethoux (1979) differs greatly from all the previous estimates. The very large difference in the RSOW outflow from October to December (Table 1) can be attributed to his assumption that all the GAIW that entered the Red Sea during the summer season must exit as an intermediate outflow in the following months. All of the direct and indirect estimates described here are summarized in Table 1.

The most complete in space and time investigation of the exchange flow at the strait of Bab el Mandeb was carried out during 1995-1996 (Murray and Johns, 1997). It lasted 18 months and resolved accurately the velocity, temperature and salinity structure in the strait. It is the first time that the complete seasonal cycle is captured with one set of direct observations. Murray and Johns (1997) confirmed most of the earlier deductions on the seasonal cycle of the exchange flow and showed that the transition between the two-layer winter exchange to the three-layer summer exchange is a robust feature of the seasonal flow pattern. The biggest advantage of this new data is that this pattern can be quantified and several important details, such as the RSOW outflow during summer, are clear. The annual mean RSOW outflow, which is a good measure of the overall strength of the exchange, was estimated at $0.36Sv$ but showed a large annual cycle ranging from over $0.6Sv$ during the peak of the winter (February) to less than $0.1Sv$ during the peak of the summer season (August). The reversal of the surface flow and the intrusion of GAIW lasts four months (June to September) when an average of $0.22Sv$ of GAIW enter the Red Sea basin. The monthly mean values of the layer transport are plotted in Figure 1 and compared with earlier observations and indirect estimates.

The basic features of the seasonal exchange cycle between the Red Sea and the Indian Ocean can now be taken as well defined and quantified, yet there is still a poor understanding of what causes this seasonal cycle. Specifically, what are the roles of the seasonal wind and buoyancy forcing fields in the exchange? The present paper focuses on the mechanisms involved in the observed variability using an Oceanic General Circulation Model (OGCM) approach, with the goal to assess the relative importance of the different processes and forcing fields.

Model Configuration and Experiments

The available data that can be used to investigate the dynamics governing the circulation in the region are very sparse in space and time with the exception of the recent observations in the strait. This is one of the reasons for the numerous simplifications and assumptions used in all the hypotheses and models proposed to explain the Red Sea circulation and exchange with the Indian Ocean, and the qualitative nature of their findings. The Red Sea has usually been treated as a two-dimensional basin driven by idealized atmospheric forcing of only the wind-stress or thermohaline type. A more complete and quantitative approach should include a three-dimensional numerical model of the Red Sea. In this paper, we follow such an approach and perform a series of experiments using different combinations of wind stress and buoyancy forcing to resolve their respective roles in the mean exchange with the Indian Ocean and its seasonal cycle. Since the primary goal is to examine the effect of the different forcing mechanisms, and since detailed data are available only at Bab el Mandeb, it is desirable to include the strait within the model domain as a point of comparison between model results and observations, rather than using it as a boundary. Furthermore, important processes taking place outside the basin that may affect the exchange flow have been proposed, such as the wind-induced upwelling in the northwestern Gulf of Aden (Patzert, 1974a). Therefore, the domain chosen for numerical experiments includes a part of the Gulf of Aden (Figure 2).

The numerical experiments were carried out with the Miami Isopycnic Coordinate Ocean Model (MICOM) (Bleck et al., 1992; Bleck and Chassignet, 1994). The most important difference of MICOM compared with other models is that it has a vertical discretization in layers of constant potential density. On the top of the isopycnic layers there is a thermodynamically active mixed layer of the Kraus-Turner type (Kraus and Turner, 1967; Gaspar, 1988), which is vertically homogeneous but of varying density in the horizontal.This layer provides the connection between the atmospheric forcing and the interior domain. The annual cycle of the atmospheric forcing causes the mixed layer to expand and shrink and thus to exchange properties with the interior layers which can outcrop in the mixed layer by becoming massless.

The horizontal grid is defined on a Mercator projection with the grid size fixed in the longtitudinal direction but varying with the cosine of latitude. In the experiments presented here a horizontal grid interval of 0.1^o (or about $10km$) was chosen in order to resolve the very narrow channel at Bab el Mandeb. The two gulfs in northern end of the Red Sea (Suez and Aqaba) are very small with very complicated topography and were not explicitly included in the present experiments. The domain is extended outside the Red Sea to incorporate part of the Gulf of Aden reaching the 45^oE. There are several reasons for including the western part of the Gulf of Aden and the Bab el Mandeb in the domain. The strait of Bab el Mandeb is the only open boundary of the basin where advective freshwater and heat fluxes can occur to balance the air-sea fluxes over the basin. The dynamics of the region including the formation processes are reflected in the exchange flow at the strait. Furthermore, since the most comprehensive available data set comes from the area of the strait, it is the best point for validation of the results of the numerical simulation. Another reason for including the western Gulf of Aden in the domain is that important water masses and dynamics involved in the seasonal circulation may be located in the area outside the Red Sea basin (e.g., Patzert, 1974a).

The vertical density structure is defined by 6 isopycnic layers and a mixed layer, shown in Table 2. The number and densities chosen for the layers used in these experiments take into account all the basic water masses and the strong pycnocline located at the base of the mixed-layer, so that the model can reproduce the basic density structure observed and involved in the Red Sea circulation. The distinction between water masses must take into account the temperature and salinity characteristics, since the density stratification does not always reflect the presence of a certain water type. Bottom topography and coastlines were obtained from the ETOPO5 digital data set with $5'$ resolution by averaging the topographic data located in each 0.1^o grid box. A correction was applied in the area of the strait where ETOPO5 data had a maximum sill depth of about 100 m which is 60 m shallower than the 160 m sill depth at the Hanish Sill (Murray and Johns, 1997). At the open end of the domain, in the Gulf of Aden, a 0.5^o buffer zone was added in which hydrography is relaxed towards monthly values derived from the Levitus (1982) climatology, with a relaxation time of 60 days.

Both mechanical and thermodynamic forcing are used to drive the model. The momentum flux is given by the components of the wind stress. The along-axis component of the wind stress derived from COADS is plotted in Figure 3 as a function of latitude, for January and July (the months that coincide with the peak of the winter and summer season, respectively). The most interesting feature is the seasonal reversal of the wind stress in the southern Red Sea. The thermodynamic forcing consists of the heat flux and the freshwater flux (which is imposed as a virtual salt flux, Bleck et al., 1992) and the mixed layer is stirred by turbulence generated by the oceanic friction velocity and the buoyancy flux. The atmospheric forcing functions applied to the model are derived from COADS (da Silva et al., 1994) but with several adjustments. Sofianos et al. (2001) derived constraints on the annual mean heat and freshwater budgets of the Red Sea, using the observed heat and salt fluxes at the strait, which give 11 Wm^{-2} heat loss and $2.06 myear^{-1}$ $E-P$, respectively. The COADS data yield a heat gain of 90 Wm^{-2} and a $1.5 myear^{-1}$ $E-P$ for the Red Sea basin. These values are considerably different from the observed values and cannot be expected to yield reasonable results for the modeled exchange flow if used as is. The heat gain of 90 Wm^{-2} from COADS, in particular, is approximately 100 Wm^{-2} greater than the heat loss of about 10 Wm^{-2} obtained from observations. The first correction applied is an addition of $0.5 myear^{-1} E-P$ uniformly in space and time throughout the year. While in reality it is unlikely that this correction is uniform in space or time, it is not clear what its spatial or seasonal variations should be, and therefore the simplest approach is taken. After adding the latent heat produced by this correction term in the heat flux (each 0.5 $m/year$ of evaporation corresponds to approximately 40 Wm^{-2} of heat loss) we need another $60 Wm^{-2}$ of heat loss to the atmosphere, which is added again uniformly in space and time since the spatial distribution and the seasonal cycle of the air-sea fluxes over the Red Sea involve great uncertainties. Thus, we are effectively assuming that the spatial and temporal (monthly) patterns in the air-sea fluxes over the region from COADS are valid but with a constant bias. The seasonal cycles of $E-P$ and heat flux from COADS, after applying the corrections, are plotted in Figure 4. The model experiments were initialized using the National Oceanic Data Center (NODC) hydrographic data for the winter state (Figure 5).

Six experiments were carried out using the same model configuration but differing in the application of the forcing fields or in the buffer zone implementation, as summarized in Table 2. The first one (E1) is the most "realistically" forced experiment and includes seasonal wind and buoyancy forcing and a seasonally varying hydrographic profile at the Gulf of Aden buffer zone. The goal of this experiment is to capture as much variability of the exchange flow as possible, to serve as a reference experiment for all the other experiments. The next two (E2 and E3) include only one driving field, either wind or thermohaline forcing, to investigate the different role and importance of each one on the exchange flow. Without any buoyancy loss in E2, the basin is no longer a concentration basin and the exchange is not of the inverse estuarine type and cannot be compared with observations and other experiment results. To avoid this, another experiment (E4) is carried out where the seasonal wind forcing is combined with steady (annual mean) thermohaline forcing. In the fifth experiment (E5) the opposite combination was chosen (annual mean wind forcing and seasonally varying thermohaline forcing). Finally, a diagnostic experiment was performed (E6), where hydrography in the buffer zone is relaxed towards the annual mean (no seasonal variability present in the buffer zone), to investigate the influence of the buffer zone on the variability of the exchange flow.

The wind- and/or thermohaline-driven circulations develop rapidly, and the flow acquires its basic characteristics after the first few months of adjustment. Fully equilibrated solutions have not been obtained, and long term adjustments, different for each simulation, are still taking place at the end of the simulations, associated with the heat and fresh water fluxes into the model interior driven by transformations occurring within the buffer zone. Nevertheless, after the first few months of simulation the pattern and strength of the exchange through the strait of Bab el Mandeb and its annual cycle changes little. All the experiments were carried out for 10 years and the results presented in the next section are an average of the last 9 years of the model integrations.

Model Results

The exchange flow produced in the experiments E1, E3 and E4 will be presented and compared with the recent observations at the Bab el Mandeb (Murray and Johns, 1997). The model data are taken from the location in the model equivalent to the Perim Narrows at the southern end of the Bab el Mandeb, which is where the Murray and Johns (1997) observations were conducted. In all the numerical simulations the most active layers in the area of the strait, and those in which most of the volume transport of inflow and outflow is taking place, are the surface layer (the mixed layer), the second layer representing the GAIW, and the sixth layer which comprises the core of the RSOW outflow. Although the other 4 layers produce much smaller transports, they are also included in the exchange estimates according to their temperature and salinity characteristics and the direction of the flow in them. In order to compare the model results with the layer transports available from observations, the mixed layer is taken to represent the surface layer (the inflow layer in winter and shallow outflow layer in summer), layers 2 and 3 represent the GAIW water intrusion (these layers disappear during winter inside the basin when the mixed layer deepens due to atmospheric forcing), and the layers below this (layers 4, 5, 6, and 7) comprise the hypersaline outflow at the bottom of the strait ($39.8psu$ from the model results compared to $39.7psu$ from observations (Murray and Johns, 1997)).

The three-layer transports from the first experiment (E1) are plotted in Figure 6. Although some differences with the observations do exist, as described below, the basic conclusion is that the model is able to capture the seasonal pattern of the exchange flow. There is a reversal of the surface flow during summer, accompanied by weaker RSOW outflow. At the same time a strong intermediate inflow is present with an average transport of $0.23Sv$. Furthermore, the strength of the exchange is of the correct order of magnitude, with an annual mean RSOW outflow of $0.38Sv$ (compared with the $0.36Sv$ obtained from observations).

The most important differences between the model and the observations are in the time when the peaks of the seasonal exchange take place, and the range of the seasonal cycle. The peak of the summer season (represented by the reversal of the surface flow, the maximum of the intermediate intrusion and the minimum of the RSOW outflow) takes place during June in the model instead of August as suggested by observations (Figure 1). The amplitude of the seasonal cycle, for both the surface layer and RSOW layer (and particularly the latter), is smaller than the observations. These discrepancies can arise for several reasons which may include aspects of the model configuration and problems in the atmospheric forcing fields. Also, we do not know if the period of the observations is a typical one, in the sense that it can be represented by the climatological data sets used for driving the model simulations and relaxing the buffer zone (COADS and Levitus). Overall, this experiment is quite successful, reproducing the the main features and the strength of the exchange flow. Therefore, it is useful to consider the other two experiments (thermohaline- and wind-driven) to investigate the specific roles of the forcing mechanisms.

Experiment E3 includes seasonal thermohaline forcing but no wind forcing. Although no wind forcing is applied, the strength of the exchange does not change perceptibly (Figure 7). The annual mean RSOW outflow is now $0.39Sv$, almost identical to the previous result and the observations. However, the seasonal cycle is substantially changed with the RSOW outflow now showing little variation throughout the year. The surface and intermediate layers still show a strong seasonal cycle, but the surface flow never reverses in summer and the intermediate intrusion continues beyond the summer into late fall. The overall strength of the GAIW intrusion is similar in magnitude to that found in experiment E1 despite the differences in amplitude and phase.

The exchange flow from experiment E4, forced by the seasonal wind-stresses and the annual mean thermohaline fluxes, is presented in Figure 8. The first and perhaps most striking result is the reduction in the overall strength of the exchange. The annual mean RSOW outflow is now $0.23Sv$, 40% weaker than in the case of the full forcing experiment (E1). In general, the flow at the strait is much weaker than the previous two experiments and more irregular. Nevertheless, some of the characteristics of the seasonal exchange cycle are evident in this simulation. The summer reversal of the surface flow, although very weak, does exist during July and at the same time the intermediate inflow acquires its maximum. The RSOW outflow also seems to respond at this time, becoming slightly weaker, but it remains weaker even into the fall when the surface inflow resumes and the intermediate intrusion decays.

The response of the Red Sea to the combined effects of thermohaline and mechanical forcing is not expected to be linear. One way to investigate this is to compare the results of experiment E1, forced with both the seasonal wind and thermohaline fields, with the sum of the exchange flow produced by the experiments involving the seasonal winds only (E2) and the seasonal thermohaline forcing only (E3). The comparison is presented in Figure 9. The obvious differences of the two results show that the final outcome is not a simple linear addition of the two effects. While the summer intrusion of GAIW is reproduced, the surface flow does not reverse in the summer nor does the deep outflow show a significant reduction in summer. The wind and thermohaline forcing are connected and interact such that their combination produces an exchange flow similar to the observed one.

Since the general circulation of the whole domain ends at the buffer zone which also provides the necessary supply of fresh water to compensate the huge evaporation rate, special attention must be given to the influence of the variability in the buffer zone on the variability of the flow at the strait. With this in mind the last experiment (E6) was carried out, where the hydrography is held constant with the annual mean values at the outer edge of the buffer zone. Apart from some minor differences in the temperature and salinity characteristics of the water masses taking part in the exchange flow (not shown), which arise from the constant values of temperature and salinity used in the buffer zone, the result is the same as for the full forcing experiment (E1). Thus, although the water masses present in the Gulf of Aden play an important role in the circulation and the heat and fresh water budgets of the Red Sea, the variability in seasonal stratification far away from the strait does not seem to greatly influence the dynamics of the Red Sea.

There are some special issues that can be addressed using the model results. One of the most interesting of these is the mechanism by which the summer wind field contributes to or controls the surface flow reversal. Namely, what is the relative importance of the direct wind-stress compared to its indirect effects (via wind-induced upwelling in the northwestern Gulf of Aden which may lower the sea level outside the basin and produce a surface pressure gradient driving surface waters from the Red Sea, as proposed by Patzert (1974a))? To investigate this question the sea surface elevation difference between the the two ends of the strait and the wind-stress influence on the surface layer were computed and compared in the momentum equation

$$\frac{\partial u}{\partial t} = -g\frac{\partial \eta}{\partial x} + \frac{\tau^x}{\rho H} \tag{1}$$

where H and ρ are the thickness and density of the surface layer. The two terms on the right hand side were computed at the time of the summer reversal and the acceleration that can be produced from each one was estimated. The ratio of the two terms is $O(1)$, so that we can conclude that direct and indirect influence of the wind are of equal importance in the model. Furthermore, as shown in Figure 10, the upward displacement of the subsurface isopycnals at the same time in the northwestern Gulf of Aden produces a pressure gradient to drive the intermediate layers (representing the GAIW) inside the basin.

Summary and Discussion

As expected, the answer to the question of what is driving the seasonal exchange flow at Bab el Mandeb is not simple and straightforward. Both wind and thermohaline forcing are important and contribute to the seasonal variability observed. Their combination is not a simple linear addition but they interact to produce the final pattern. For example, the peak of the winter two-layer exchange in the thermohaline-driven experiment takes place during February, in the wind-driven experiment during April, and when the two forcings are combined it occurs during December. Thus it is the combination of the two that generates the circulation and sets up the proper pressure gradients capable of driving the seasonal cycle of the flow at the strait. The wind forcing seems to be most influential in controlling the seasonal changes, such as the reversal of the surface flow and the abrupt commencement of the GAIW intrusion. However, a strong reduction of the surface inflow during summer appears to be related to buoyancy forcing. Without this effect the wind driven reversal in summer would be either very weak or perhaps not occur at all. Some of the irregularities present in the wind-driven result, especially during the fall, can perhaps be attributed to the very weak wind field of COADS in the end of the summer and beginning of fall (August to October). Although the annual mean heat and freshwater budgets are known with accuracy, the seasonal variability of the different terms involved in the buoyancy flux include large uncertainties and some of them are highly disputed. The weaker seasonal cycle in the thermohaline-driven experiment (E3) and the prolonged summer type of exchange might be explained by the uncertainty in the seasonal range of this forcing mechanism. Recall that the corrections in the heat flux and $E-P$ were added uniformly around the year, although it is possible (and likely) that they could contribute to a stronger seasonal variability.

A very striking result of the experiments is the influence of the separate forcing mechanisms on the mean exchange flow and especially the large reduction in the strength of the total exchange for experiment E4, which has seasonal wind forcing but steady (annual mean) thermohaline forcing. The annual mean RSOW outflow is reduced to almost half its value in experiment E1 even though the same average buoyancy loss is used in driving the model. The seasonal variability of the thermohaline forcing therefore seems to be very important in producing the observed magnitude of the annual mean exchange. This must be closely related to the amount of RSOW formed in the basin which in turn should be related to the maximum buoyancy loss during the peak of the winter when the layers of RSOW are formed. Without a strong winter peak in the buoyancy loss to the atmosphere, especially in the northern part of the Red Sea, the amount of RSOW formed is not enough to account for the observed values. Furthermore, the circulation produced in the simulations including the seasonal cycle of the buoyancy flux (E3 and E5) exhibit a more vigorous basinwide circulation (Sofianos and Johns, 2001) than the one produced by the respective experiments including only the seasonal cycle of the wind-stress forcing (E2 and E4).

Although there is no intention here to discuss details of the circulation inside the Red Sea (for a description of the results of the model concerning the three-dimensional circulation in the Red Sea, the reader is referred to Sofianos and Johns,2001), it is important to give an idea of the overturning circulation in the model that produces the exchange flow at the strait. Since MICOM is a layered model, the overturning circulation is plotted on the σ_θ-latitude plane, and is presented in Figure 11 for experiment E1 for the months of December (the peak of the winter season when the strongest two-layer exchange is taking place) and June (when the strongest surface outflow is present in the model). Although during December the production of RSOW does not achieve its maximum, which takes place one to two months later (see Sofianos and Johns, 2001), the two-layer cellular circulation is well established (Fig. 11a). A single broad recirculation cell is present in winter centered at about 17^oN. Most of the fluid (about 2/3) sinks in the northern Red Sea north of 22^oN. A small amount of upwelling from the 2nd and 3rd layers into the mixed layer occurs south of 17^oN within the Red Sea.

The summer overturning circulation presents two cells, a shallow one in the southern part of the basin and a deeper one centered in the middle of the basin (about 20^oN, Fig 11b). The shallow cell is associated with the reversal of the surface flow and the GAIW intrusion, in which water entering the basin in the GAIW layer upwells south of 20^oN to feed the shallow outflow. The second, deeper, cell connects the intermediate inflow with the RSOW outflow, which is about half the strength in summer as it is in winter. Some recirculation within the basin also occurs in the deeper cell. We have to emphasize here that the numerical model result for RSOW outflow, although very close to the observations on the annual mean, presents a weaker annual cycle than observed and the summer RSOW outflow is overestimated.

In summary, the experiments conducted here have been successful in reproducing the basic features of the observed seasonal exchange between the Red Sea and the Indian Ocean, and give some insight into the forcing mechanisms responsible for this annual cycle. Modeling of the Red Sea remains a challenging task because there are several uncertainties in the atmospheric fields to drive such a model and very few data to compare against the model results away from the strait. The development of reliable forcing data sets is one of the most important needs to further improve our understanding of the Red Sea circulation and exchange with the Indian Ocean. Future modeling attempts could also investigate the higher frequency variability which may play an important role in the dynamics and is not considered here.

Acknowledgments. This work is supported by Office of Naval Research contract N00014-95-1-0025 to the University of Miami. The authors are indebted to Eric Chassignet, Linda Smith, and Afonso Paiva for their help in configuring the model for the Red Sea and for numerous discussions.

References

Bethoux, J. P., 1979, Budgets of the Mediterranean Sea. Their dependence on the local climate and the characteristics of the Atlantic waters, *Oceanol. Acta, 2,* 157-163.

Bethoux, J. P., 1987, Variabilite climatique des echanges entre la Mer Rouge et l'Ocean Indien, *Oceanol. Acta, 10,* 285-291.

Bleck, R., C. Rooth, D. Hu, and L. T. Smith, 1992, Salinity-driven thermocline transients in wind- and thermohaline-forced isopycnic coordinate model of the North Atlantic, *J. Phys. Oceanogr., 22,* 1486-1505.

Bleck, R., and E. P. Chassignet, 1994, Simulating the oceanic circulation with isopycnic-coordinate models, in: *The Oceans: Physical-chemical dynamics and human impact,* S. K. Majumar, E. W. Miller, G. S. Forbes, R. F. Schmalz, and A. A. Panah eds., The Pennsylvania Academy of Science, Pennsylvania, 17-39.

da Silva, A. M., C. C. Young, and S. Levitus, 1994, Atlas of surface marine data 1994. Volume 1: Algorithms and procedures. *NOAA Atlas NESDIS 8,* U. S. Department of Commerce, NOAA, NESDIS, 83 pp.

Gaspar, P., 1988, Modeling the seasonal cycle of the upper ocean, *J.Phys. Oceanogr., 18,* 161-180.

Hastenrath, S., and P. J. Lamb, 1979, Climatic Atlas of the Indian Ocean, Univ. Wisconsin Press, Madison.

Kraus, E. B., and J. S. Turner, 1967, A one-dimensional model of the seasonal thermocline. II. The general theory and its consequences, *Tellus, 19,* 98-105.

Krümmel, O., 1911, Handbuch der Ozeanographie, 2, Stuttgard.

Levitus, S., 1982, Climatological atlas of the world ocean, *NOAA Prof. Paper No 13,* U. S. Govt. Printing Office, 173 pp.

Luksch, 1901, Expedition S. M. POLA in das Rota Meer, nordliche Halfte (October 1895 - Mai 1896). Wissenschaftliche Ergebnisse, physikalische Untersuchungen, *Denkschrift d. kaiserl. Akad. Wissensch. in Wien, 69,* 337pp.

Maillard, C., and G. Soliman, 1986, Hydrography of the Red Sea and exchanges with the Indian Ocean in summer, *Oceanol. Acta, 9,* 249-269.

Maury, M. F., 1855, The physical geography of the sea and its meteorology, The Harvard Library, Cambridge, Mass, 432 pp.

Murray, S. P., and W. Johns, 1997, Direct observations of seasonal exchange through the Bab el Mandeb strait, *Geophys. Res. Let., 24,* 2557-2560.

Neumann, J., 1952, Evaporation from the Red Sea, *Israel Explor. J., 2,* 153-162.

Neumann, A. C., and D. A. McGill, 1962, Circulation of the Red Sea in early summer, *Deep-Sea Res., 8,* 223-235.

Patzert, W. C., 1974a, Wind-induced reversal in Red Sea circulation, *Deep-Sea Res., 21,* 109-121.

Patzert, W. C., 1974b, Volume and heat transports between the Red Sea and Gulf of Aden, notes on the Red Sea heat budget, in: *L'oceanographie physique de la Mer Rouge,* CNEXO, Paris, 191-201.

Phillips, O. M., 1966, On turbulent convection currents and the circulation of the Red Sea, *Deep-Sea Res., 13,* 1149-1160.

Privett, D. W., 1959, Monthly charts of evaporation from the Indian Ocean (including the Red Sea and the Persian Gulf), *Q. Jl. R. Met. Soc., 85,* 424-428.

Schott, G., 1929, Uber die Wasserbewegungen im Bab el Mandeb, *Ann. d. Hydrog., 62,* 10-14.

Sewell, R. B. S., 1934, The John Murray Expedition to the Arabian Sea, *Nature, 133,* 86-89.

Siedler, G., 1968, Schichtungs- und Bewegungsverhaltnisse am Sudausgang des Roten Meeres, *"Meteor" Forschungsergebn, A(4),* 1-76.

Siedler, G., 1969, General circulation of the water masses in the Red Sea, in: *Hot brines and recent heavy metal deposits in the Red Sea,* E. T. Degens and D. A. Ross eds., New York, 131-137.

Sofianos, S. S., 2000, Circulation and water mass formation in the Red Sea, and the exchange with the Indian Ocean, PhD Thesis, University of Miami.

Sofianos, S. S., W. E. Johns, and S. P. Murray, 2001, Heat and freshwater budgets in the Red Sea from direct observations at Bab el Mandeb, *Deep-Sea Res.*, (in press).

Sofianos, S. S., and W. E. Johns, 2001, An OGCM investigation of the Red Sea circulation. Part II.: The three-dimensional circulation in the Red Sea, *J. Geophys. Res.*, (submitted).

Thompson, E. F., 1939a, Chemical and physical investigations. The general hydrography of the Red Sea, *John Murray Expedition 1933-34, Scientific Reports, 2,* 83.

Thompson, E. F., 1939b, Chemical and physical investigations. The exchange of water between the Red Sea and the Gulf of Aden over the "Sill", *John Murray Expedition 1933-34, Scientific Reports, 2,* 105.

Tragou, E., and C. Garrett, 1997, The shallow thermohaline circulation of the Red Sea, *Deep-Sea Res., 44,* 1355-1376.

Tragou, E., C. Garrett, R. Outerbridge, and G. Gilman, 1999, The heat and freshwater budgets of the Red Sea, *J. Phys. Oceanogr., 29,* 2504-2522.

Vercelli, E., 1927, Richerche di oceanografia fisica eseguite della R. N. AMMIRAGLIO MAGNAGHI (1923-24), Part IV. La temperatura e la salinita, *Annali Idrografici, 11,* 1-66.

Vercelli, E., 1931, Nuove richerche sulli correnti marine nel Mar Rosso, *Annali Idrografici, 12,* 1-74.

Vercelli, E., 1931, Le esplorazioni talassografiche nel Mar Rosso, *Atti del Primo Congresso di Studi Coloniali,* Firenze, 23pp.

Yegorov, N. I., 1950, Calculation of the heat balance of the Red Sea, *Meteorologia igidrologia, 3,* 49-56.

S. Sofianos, Department of Physics, University of Athens, University Campus Build. PHYS-5, Athens 15784, Greece (e-mail:sofianos@oc.phys.uoa.gr)

W. E. Johns, Rosenstiel School of Marine and Atmospheric Science, University of Miami, 4600 Rikenbacker Causeway, Miami FL 33149, USA (e-mail:wjohns@rsmas.miami.edu)

Received ____________________

---

[1]Now at Department of Physics, University of Athens, Athens, Greece

Figure 1. Estimates of the monthly mean layer transport at the strait of Bab el Mandeb.

Figure 2. The domain and its bathymetry included in the OGCM experiments.The area indicated by red color is the location of the buffer zone where hydrography is relaxed to Levitus climatology.

Figure 3. The along Red Sea axis of the wind stress (in Pa) during January and July from COADS climatology.

Figure 4. Seasonal cycles of (a) freshwater and (b) heat fluxes over the model domain from COADS, after corrections in the heat and freshwater budgets of the Red Sea.

Figure 5. The initial (winter) stratification used in the OGCM experiments, produced by the NODC data set.

Figure 6. Monthly layer transport at the location of the Perim Narrows (positive represents flow into the Red Sea) produced by the full-forcing experiment (E1). The values are averages over the last 9 years of simulation.

Figure 7. Monthly layer transport at the location of the Perim Narrows produced by the thermohaline-driven (E3) experiment (average over the last 9 years of simulation).

Figure 8. Monthly layer transport at the location of the Perim Narrows from the wind-driven (E4) experiment (average over the last 9 years of simulation).

Figure 9. Comparison between the results of the full forcing experiment (E1 - thick lines) and the sum (thin lines) of the experiments E2 (seasonal winds only) and E3 (seasonal cycle of the thermohaline forcing only).

Figure 10. The pressure gradient between the two ends of the strait from the experiment E1, for winter (January) and summer (June). Positive values correspond to higher pressure in the Gulf of Aden, forcing inflow to the Red Sea. During the summer season the surface pressure gradient reverses, helping to drive the surface outflow from the Red Sea.

Figure 11. Meridional overturning volume fluxes for (a) December and (b) June, from MICOM simulation (experiment E1). Colors indicate different layers and contours indicate the overturning cells.

Table 1. Direct and indirect estimates of the layer transport (in Sv) at Bab el Mandeb (the three rows for each author correspond to the three layers, surface, GAIW intrusion and RSOW outflow, respectively).

MONTH	Vercelli	Siedler	Patzert	Maillard and Soliman	Bethoux
JAN			0.57		0.72
			0		0
			-0.54		-0.67
FEB			0.40		0.70
			0		0
			-0.37		-0.67
MAR	0.58		0.57		0.69
	0		0		0
	-0.49		-0.54		-0.67
APR			0.42		0.68
			0		0
			-0.39		-0.67
MAY			0.38		0.67
			0		0
			-0.35		-0.67
JUN			-0.06		0.67
			0.09		0
			0		-0.67
JUL			-0.20	-0.16	-0.26
			0.23	0.25	0.35
			0	-0.06	-0.09
AUG			-0.21	-0.25	-0.23
			0.24	0.33	0.35
			0	-0.05	-0.09
SEP			-0.09	-0.14	-0.20
			0.12	0.20	0.35
			0	-0.03	-0.09
OCT			0.52		0.54
			0		-0.35
			-0.49		-0.09
NOV		0.58	0.57		0.50
		0	0		-0.35
		-0.42	-0.54		-0.09
DEC			0.51		0.49
			0		-0.35
			-0.48		-0.09

Table 2. Vertical resolution (layer density) and OGCM experiments performed.

LAYER DENSITY (kgm^{-3})	EXPERIMENTS
mixed layer	full forcing (E1)
1025.75	wind forcing only (E2)
1026.25	thermohaline forcing only (E3)
1026.75	wind forcing and annual mean thermohaline forcing (E4)
1027.25	thermohaline forcing and annual mean wind forcing (E5)
1028.00	annual mean hydrography in the buffer zone (E6)
1028.60	

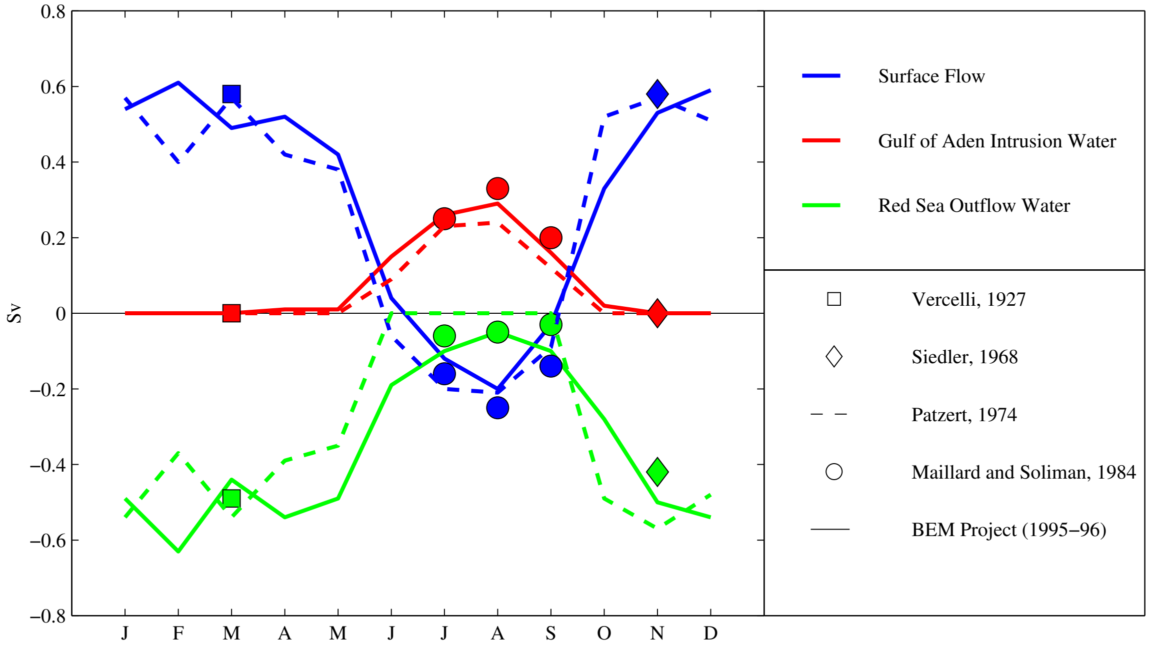

0.8
0.6
0.4
0.2
0
−0.2
−0.4
−0.6
−0.8
Sv
J
F
M
A
M
J
J
A
S
O
N
D
Surface Flow
Gulf of Aden Intrusion Water
Red Sea Outflow Water
Vercelli, 1927
Siedler, 1968
Patzert, 1974
Maillard and Soliman, 1984
BEM Project (1995−96)

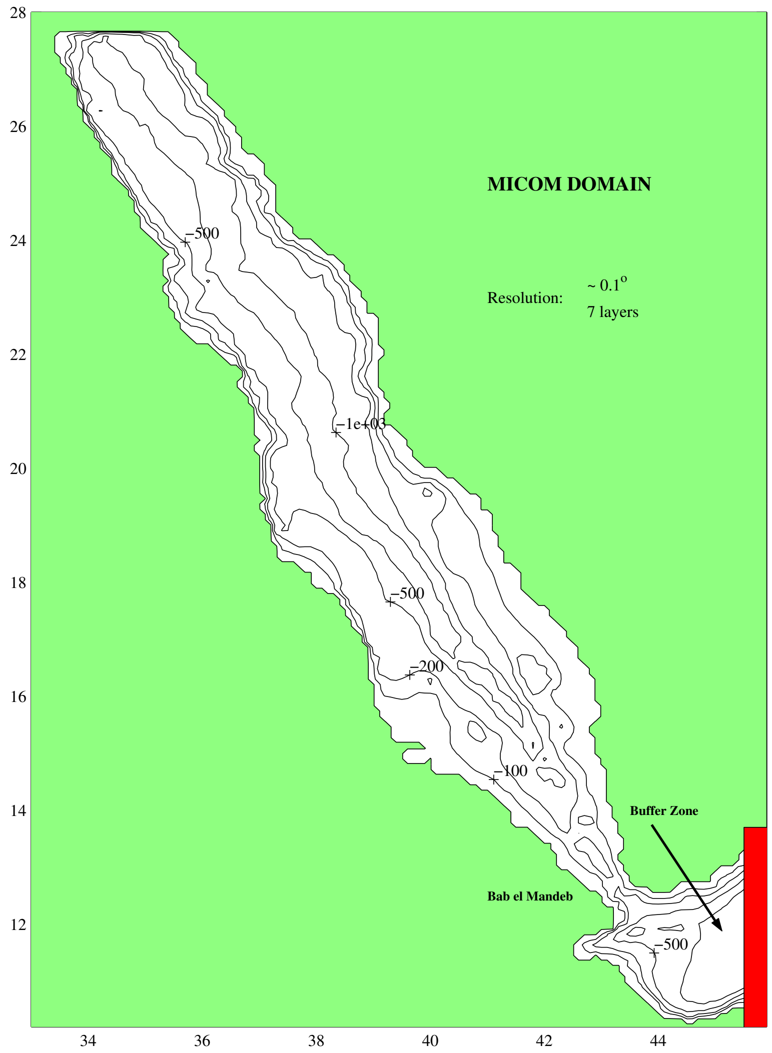

MICOM DOMAIN
Resolution:
~ 0.1°
7 layers
Buffer Zone
Bab el Mandeb
−500
−1e+03
−200
−100
28
26
24
22
20
18
16
14
12
34
36
38
40
42
44

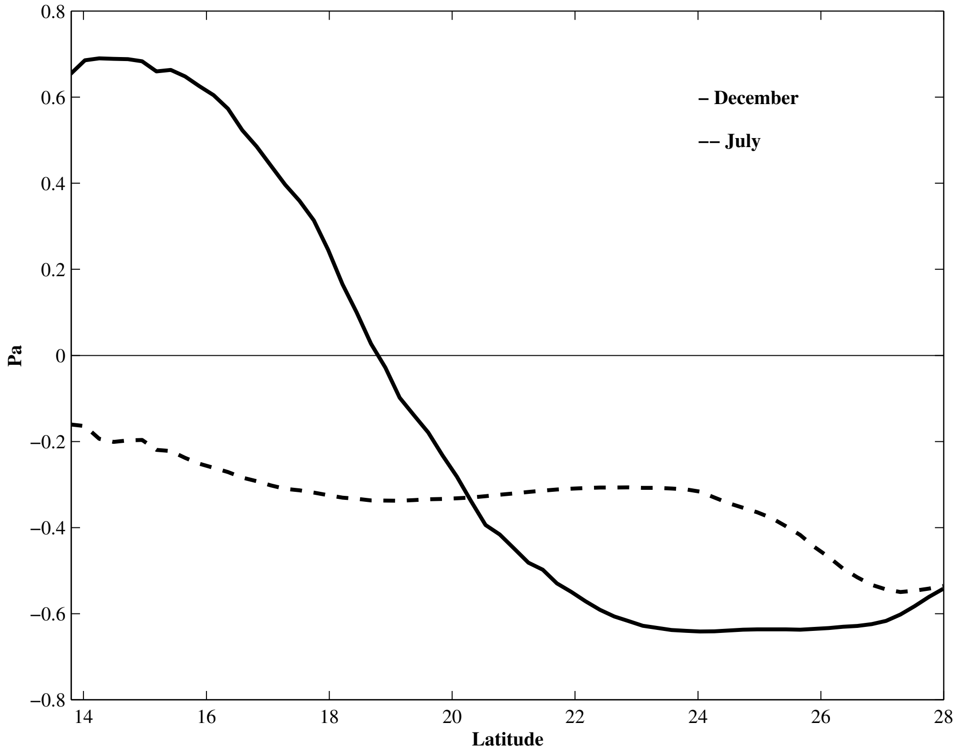

0.8
0.6
0.4
0.2
0
−0.2
−0.4
−0.6
−0.8
Pa
14
16
18
20
22
24
26
28
Latitude
– December
–– July

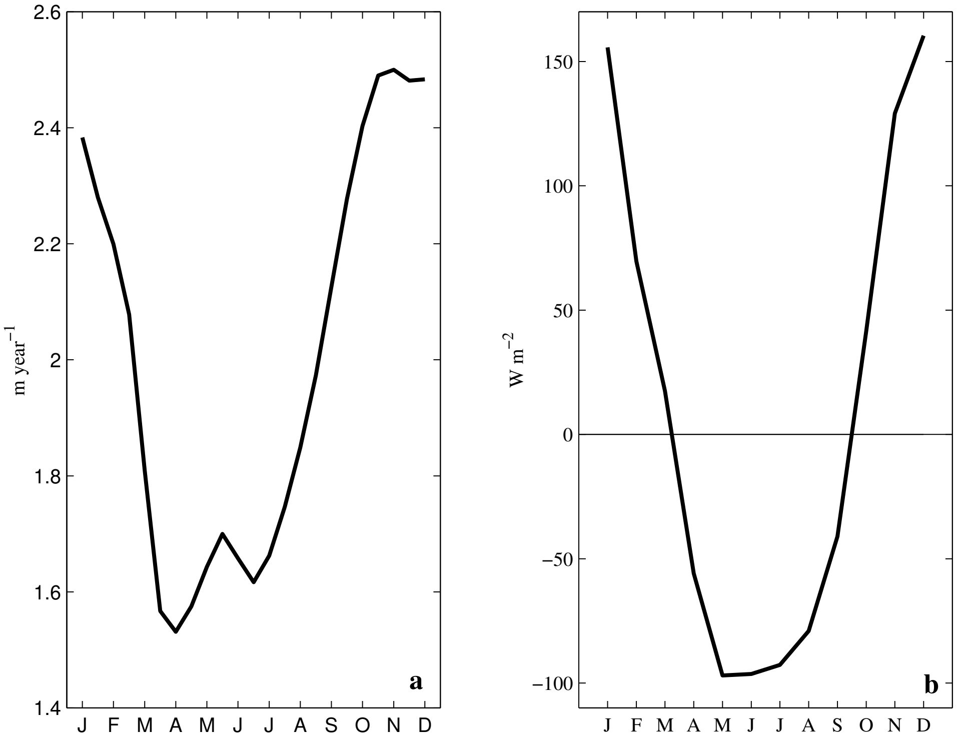
2.6
2.4
2.2
2
1.8
1.6
1.4
m year^{-1}
J F M A M J J A S O N D
a
150
100
50
0
−50
−100
W m^{-2}
J F M A M J J A S O N D
b

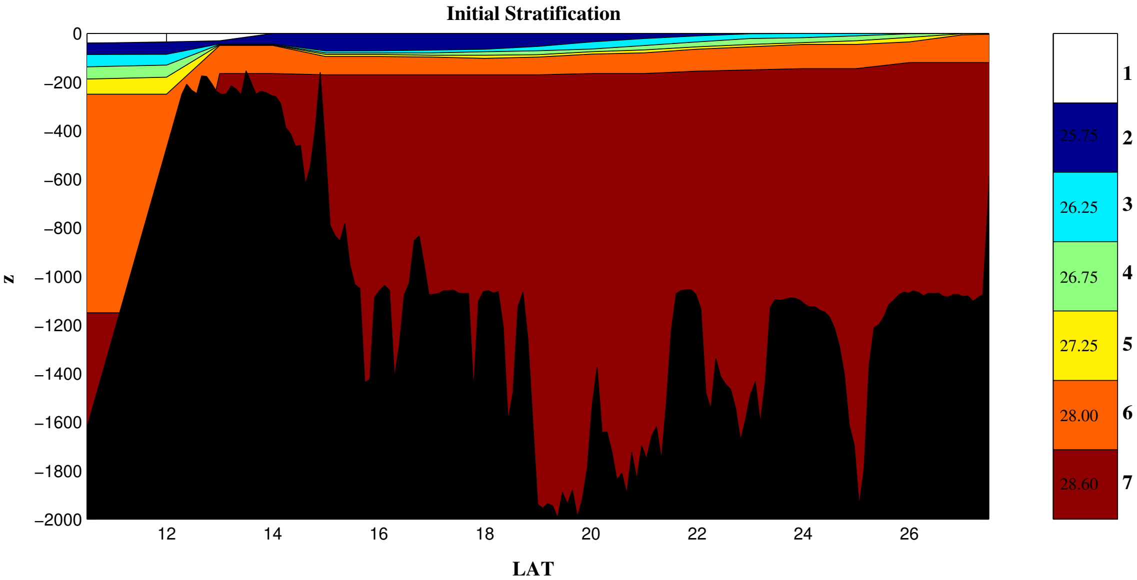
Initial Stratification
0
−200
−400
−600
−800
z
−1000
−1200
−1400
−1600
−1800
−2000
12
14
16
18
20
22
24
26
LAT
1
25.75
2
26.25
3
26.75
4
27.25
5
28.00
6
28.60
7

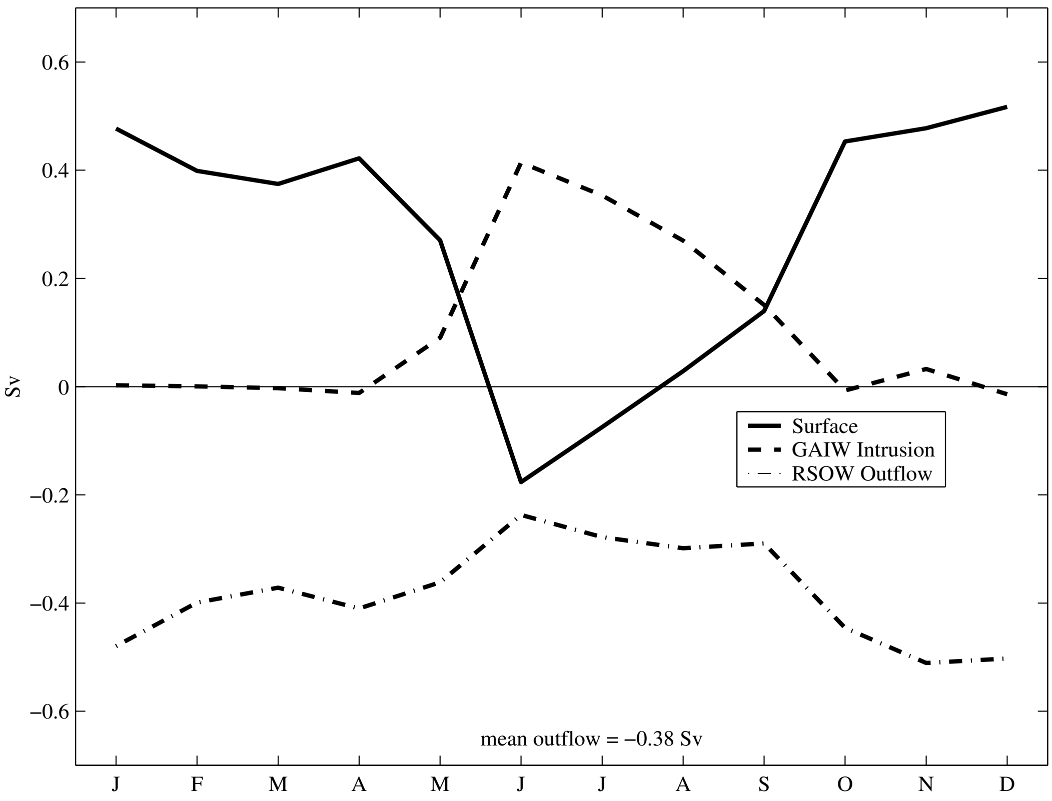

0.6
0.4
0.2
0
−0.2
−0.4
−0.6
Sv
Surface
GAIW Intrusion
RSOW Outflow
mean outflow = −0.38 Sv
J
F
M
A
M
J
J
A
S
O
N
D

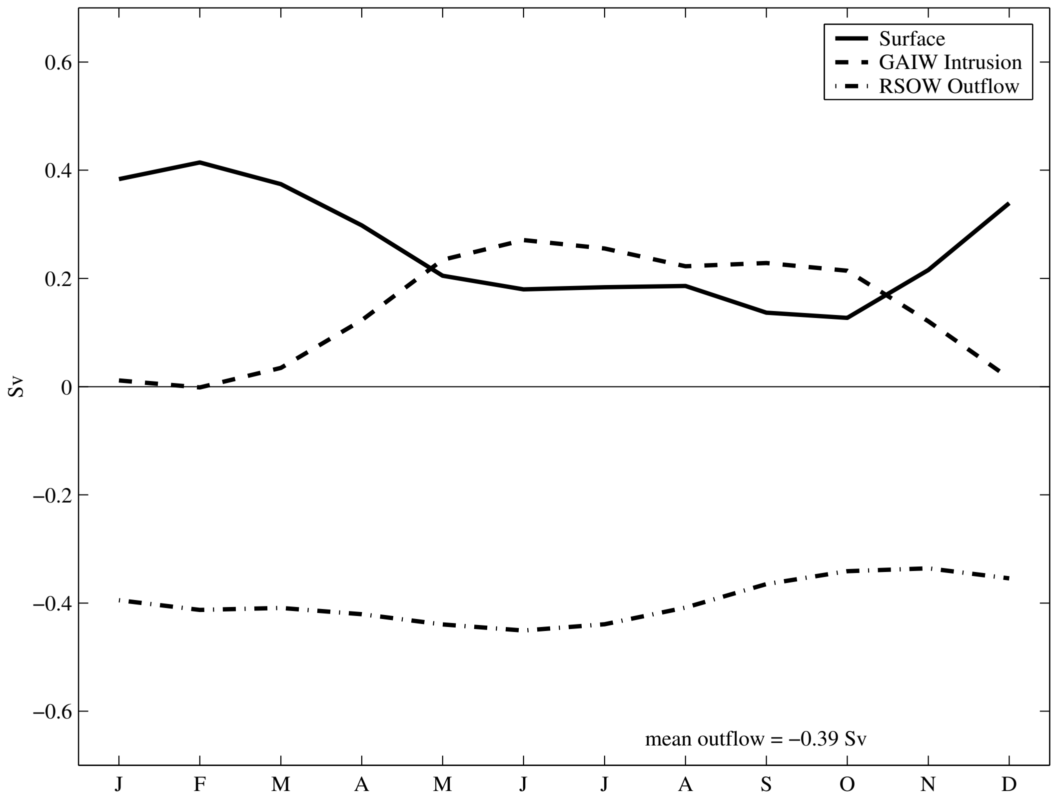
Surface
GAIW Intrusion
RSOW Outflow
0.6
0.4
0.2
0
−0.2
−0.4
−0.6
Sv
mean outflow = −0.39 Sv
J
F
M
A
M
J
J
A
S
O
N
D

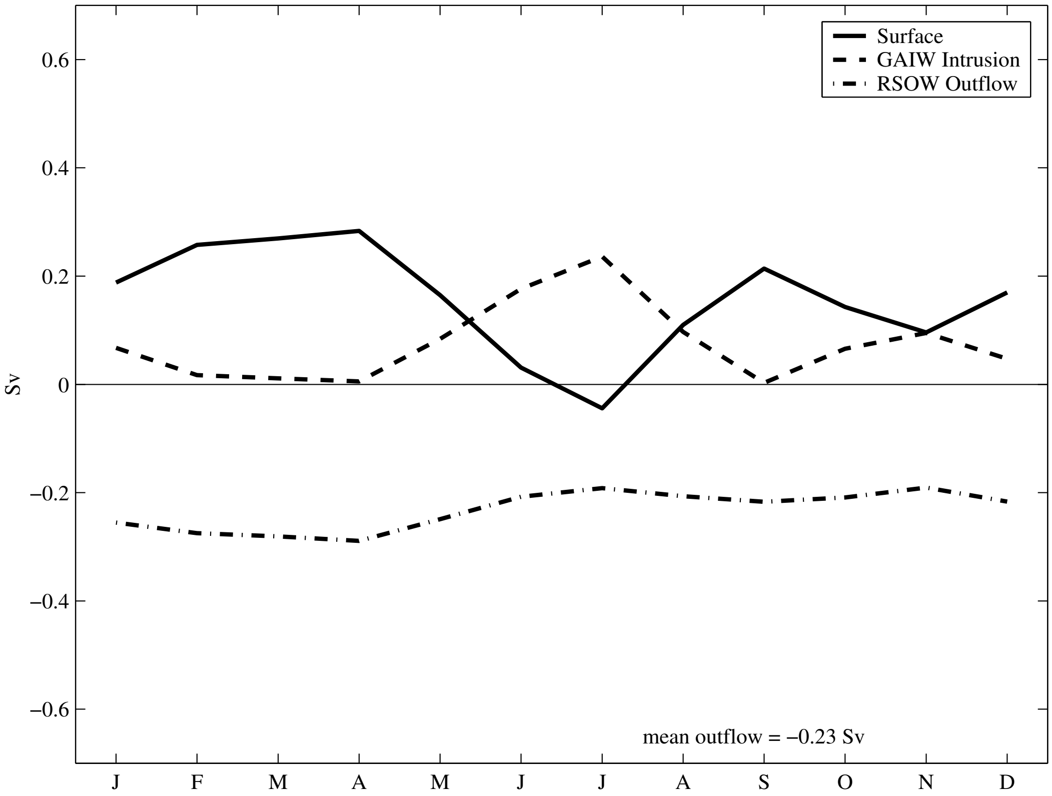
Surface
GAIW Intrusion
RSOW Outflow
0.6
0.4
0.2
0
−0.2
−0.4
−0.6
Sv
mean outflow = −0.23 Sv
J
F
M
A
M
J
J
A
S
O
N
D

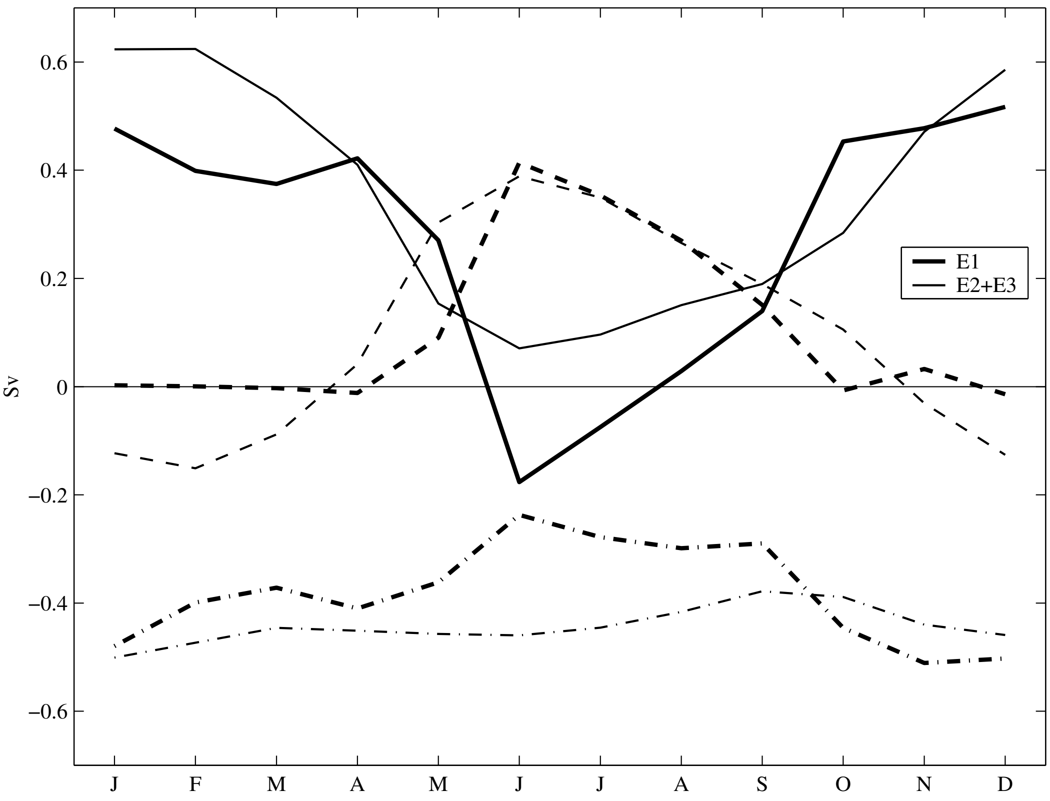
0.6
0.4
0.2
0
−0.2
−0.4
−0.6
Sv
J
F
M
A
M
J
J
A
S
O
N
D
E1
E2+E3

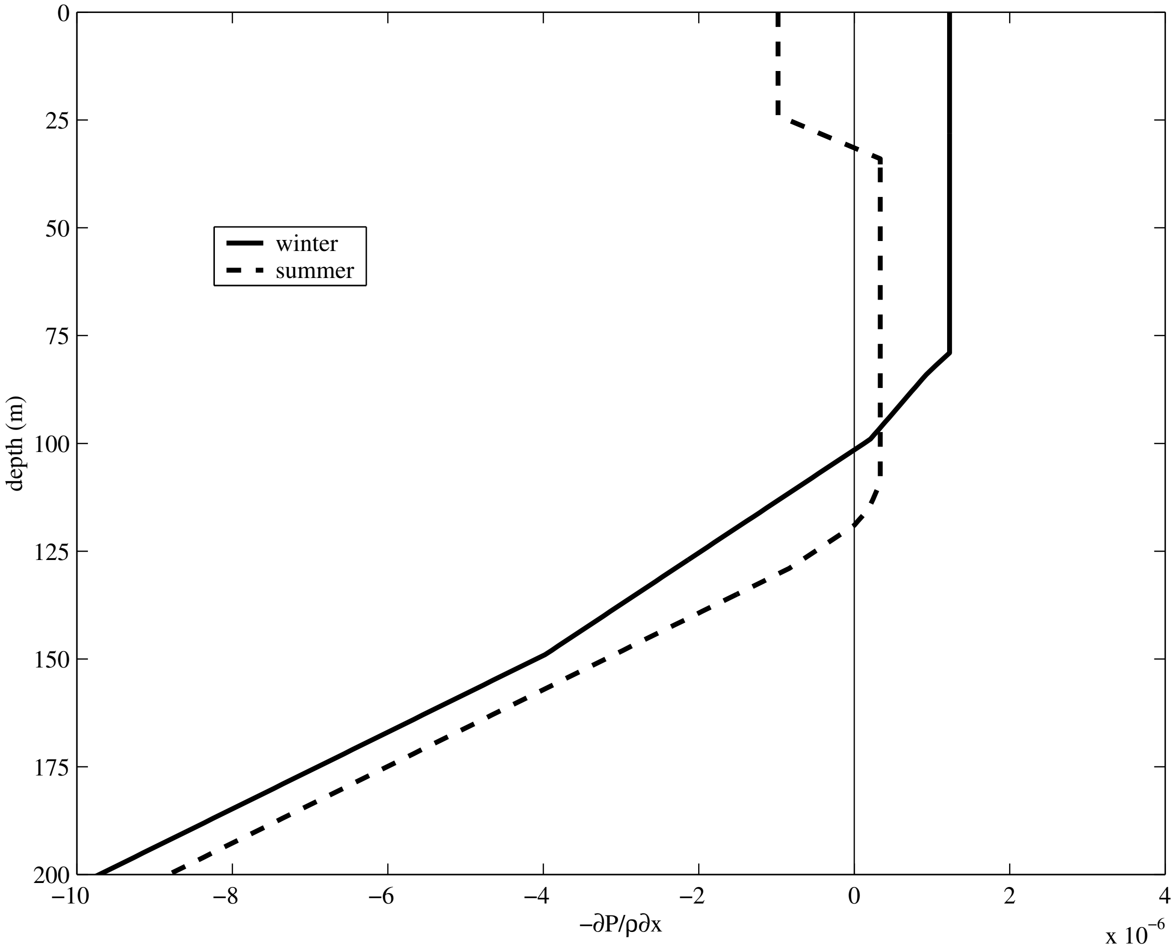

winter
summer
depth (m)
0
25
50
75
100
125
150
175
200
−10
−8
−6
−4
−2
0
2
4
−∂P/ρ∂x
x 10^{-6}

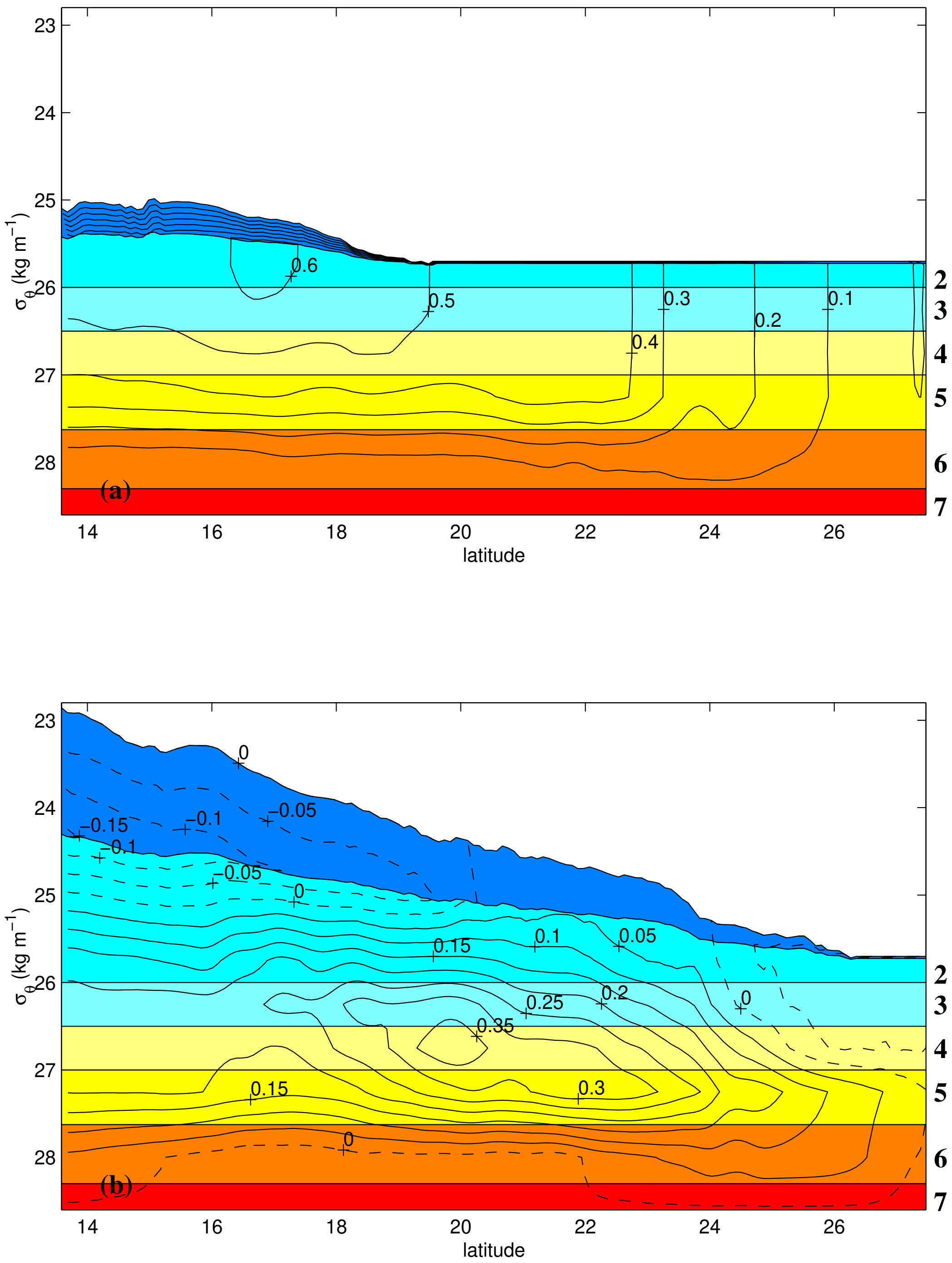

(a)
23
24
25
26
27
28
σ_θ (kg m^{-1})
0.6
0.5
0.4
0.3
0.2
0.1
2
3
4
5
6
7
14
16
18
20
22
24
26
latitude
(b)
0
−0.05
−0.1
−0.15
0.15
0.1
0.05
0.25
0.2
0.35
0.3
latitude